Microchimica Acta (2021) 188: 133
https://doi.org/10.1007/s00604-021-04788-z

ORIGINAL PAPER

Gold nanorods-based lateral flow biosensors for sensitive detection of nucleic acids

Qingcai Yu[1] · Jing Zhang[1] · Wanwei Qiu[1] · Kun Li[1] · Lisheng Qian[1] · Xueji Zhang[1,2] · Guodong Liu[1]

Received: 8 November 2020 / Accepted: 15 March 2021 / Published online: 21 March 2021

Abstract

A gold nanorod (AuNR)-based lateral flow nucleic acid biosensor (LFNAB) is reported for visual detection of DNA with a short test time and high sensitivity. AuNRs with an approximate length of 60 nm were utilized as a colored tag to label the detection DNA probe (Det-DNA). The capture DNA probe (Cap-DNA) was immobilized on the test region of LFNAB. Sandwich-type complex was formed among the AuNR-Det-DNA, target DNA (Tar-DNA), and Cap-DNA on the LFNAB by Watson-Crick base pairing. In the presence of Tar-DNA, AuNRs were thus seized on the test region of LFNAB, and the accumulation of AuNRs subsequently produced a characteristic colored band. The optimized LFNAB was able to detect 10 pM Tar-DNA without instrumentation. Quantitative analysis could be established by measuring the intensity of test band using a portable strip reader, and the detection limit of 2 pM target DNA was achieved on the LFNAB without signal amplification. The detection limit of the AuNR-based LFNAB is 250-fold lower than that of gold nanoparticle (AuNP)-based LFNABs. This work unveiled a sensitive, rapid, and economical strategy for the detection of nucleic acids, and simultaneously opening new promising routes for disease diagnosis and clinical applications.

Keywords DNA biosensor · Gold nanorods · Lateral flow · Visual detection

Introduction

The detection of DNA is remarkably essential in genetic therapy, clinical diagnostics, warning against bio-warfare agents, and a variety of biomedical studies [1–5]. The most used technique to detect DNA is polymerase chain reaction (PCR) [6, 7]. PCR is highly sensitive and accurate, but it is based on lab-bench protocols and requires relatively well-trained personnel. Moreover, false-positive results often occur in the presence of even minute amounts of fragmented DNA as contaminants [4, 8]. Therefore, the development of a facile and cost-efficient technique with high sensitivity and specificity for rapid and on-site testing of DNA is an urgent undertaking.

Lateral flow biosensors combining nanomaterials with conventional immunochromatographic assay have attracted considerable research interest on account of their excellent sensitivity, selectivity, low-cost, on-site operation, simplicity, and long-term stability [9–11]. Lateral flow nucleic acid biosensors (LFNAB) using single-strand DNA probes have recently been reported to detect specific nucleic acid sequences [2, 12, 13], bacteria [14], proteins [15], and cancer biomarkers [16]. Gold nanoparticles (AuNPs) are usually used as labels to prepare LFNABs because of their unique optical characteristics, easy fabrication, and good biocompatibility [2, 10, 17]. Unfortunately, the AuNPs-based LFNABs consistently suffer from low sensitivity and poor quantification capability because of the limited surface area of AuNPs [12, 18]. In addition, the aggregation of AuNPs-DNA conjugates often occurs in the testing and preparation of the sensors. Continuous efforts have been made to overcome these issues. For example, carbon nanotubes (CNTs) [4], horseradish peroxidase-coated

Qingcai Yu and Jing Zhang contributed equally to this work.

✉ Lisheng Qian
qianls@ahstu.edu.cn

✉ Xueji Zhang
zhangxueji@szu.edu.cn

✉ Guodong Liu
guodong.liu@ndsu.edu

[1] Institute of Biomedical and Health Science, School of Life and Health Science, Anhui Science and Technology University, Fengyang 233100, Anhui, China

[2] School of Biomedical Engineering, Shenzhen University Healthy Science Center, Shenzhen, Guangdong 518060, People's Republic of China

AuNPs [19], and AuNP-coated silica nanorods [20] have been utilized as labels to boost the LFNABs sensitivity. Although CNTs and silica nanorods provide large surface area for linking single-strand DNA probes and could be loaded with large amounts of AuNPs, controlling the length of CNTs and the numbers of AuNPs per nanorod remain massive challenges.

Recently, gold nanorods (AuNRs) have received significant research attention because of their unique electronic and optical properties [21–24]. Compared with AuNPs, anisotropic AuNRs have stronger and flexible NIR/Vis absorption and greater enabling cross-sections of surface enhancement Raman spectroscopy. Moreover, they also offer the possibility of unidirectional plasmon pervasion and enhanced photoluminescence [21]. AuNRs have been used to construct various biosensors including surface plasma resonance [25–28], fluorescent [29, 30], electrochemical [31], colorimetric [32], and plasmonic building blocks [24]. AuNRs were recently utilized as a colored tag for lateral flow immunoassay of *E. coli* O157: H7 [33].

In this study, we present an AuNR-based LFNAB for the sensitive and quantitative visual detection of DNA with a short assay time. A sulfhydryl-modified detection DNA probe (Det-DNA) was immobilized on the AuNR surface, and AuNR-Det-DNA conjugates and capture DNA probes (Cap-DNA) were used to construct the LFNAB. Sandwich-type complex was formed among the AuNR-Det-DNA, target DNA (Tar-DNA), and Cap-DNA on the LFNAB by Watson-Crick base pairing. AuNRs were thus seized on the test region of the LFNAB in the presence of Tar-DNA, and AuNRs accumulation can produce a characteristic-colored band, thus leading the visual detection of DNA without the use of any tool. After systematic optimizations, the AuNRs-based LFNAB can detect a minimum detection concentration of 2 pM target DNA, which is 250-fold beneath the detection limit of AuNP-based LFNAB. This method provides new insights into the detection of DNA and supplies top-notch results for biomedical and clinic applications.

Materials and methods

Apparatus

A cutting device called guillotine of XYZ3010 and CM3010 types dispensing platform were bought from Shanghai Jiening Biological Technology Ltd. (Shanghai, China, http://www.ivdt.cn/). A Canon camera of the 1000D EOS model was utilized to capture the pictures of LFNABs (http://www.canon.com.cn/). The portable test strip reader of DT2032 type was bought from Shanghai Goldbio Tech Co., Ltd. (Shanghai, China, http://www.goldbio.cn/). High-magnification transmission electron microscopy (TEM) images of gold nanorods were captured on a JEM-2100F instrument purchased from JEOL (https://www.jeol.co.jp/). UV-visible absorption spectra were measured by UV-3600 Spectrophotometer purchased from Shimadzu Scientific Instruments Inc. (https://www.shimadzu.com.cn/).

Reagents and materials

$HAuCl_4 \cdot 4H_2O$ and cetyltrimethylammonium bromide (CTAB) were bought from J&K Co. Ltd. (Beijing, China, https://www.jk-scientific.com/). Sodium chloride, Tween-20, sodium borohydride ($NaBH_4$), bovine serum albumin (BSA), sucrose, phosphate buffer (pH 7.4, 0.1 M PBS), 20× concentrated sodium chloride–sodium citrate buffer (SSC, 3 M NaCl in 0.3 M of sodium citrate, pH 7.0), polyvinyl pyrrolidone (PVP), sodium dodecyl sulfate (SDS), 2′-deoxyadenosine-5′-triphosphate solution (100 mM), and trisodium salt 5′ (dATP) were bought from Sangon Biotech. Co. Ltd. (Shanghai, China, https://www.sangon.com/). Nitrocellulose membranes (HFB18004), laminated cards (HF000MC100), glass fibers (GFCP000800), and cellulose fiber sample pads (CFSP001700) were bought from Shanghai Jiening Biological Technology Ltd. (Shanghai, China, http://www.ivdt.cn/).

All reagents utilized in the research were of analytical grade. The preparation of solutions was conducted with ultrapure water (18.2 MΩ·cm). The oligonucleotides utilized for the research were all bought from Sangon Biotech. Co. Ltd. (Shanghai, China), and the DNA sequences were given in the Electronic Support Materials (ESM, Table S1).

Preparation of AuNRs

AuNRs with different aspect ratios, designated AuNRs-25 (average length, 25 nm), AuNRs-60 (average length, 60 nm), and AuNRs-80 (average length, 80 nm), have been prepared according to the previous reported methods with minor modification [34–36]. The detailed syntheses procedure and scheme was given in the ESM.

Preparation of AuNR-Det-DNA conjugates

AuNRs with an approximate length of 60 nm were prepared by the above strategic approach. Next, 500 μL of AuNRs was treated with 15 μL of 1 mM dATP for 30 min with tilting rotation at room temperature (RT). Precisely 7.5 μL of 1% SDS was then added in the blend, which was hence incubated for 10 min at RT. At that point, 25 μL of 2 M NaCl and 85 μL of sulfhydryl-modified Det-DNA probe were added to the above blend, respectively. The obtained blend was hatched for 3 h at 60 °C, centrifuged at 8000 rpm for 8 min, washed three times with PBS, and re-suspended in the eluent buffer containing $Na_3PO_4 \cdot 12H_2O$, 5% BSA, 10% sucrose, and

0.25% Tween-20. The AuNR-Det-DNA conjugate solution was kept at 4 °C until utilization.

Preparation of streptavidin-biotinylated Cap-DNA and streptavidin-biotinylated Con-DNA conjugates

50 nmol of biotinylated Cap-DNA was added into 80 μL of 2.5 mg/mL streptavidin solution, and then the mixture was shaken for 1 h at 25 °C. Then adding 400 μL of PBS to the mixture, the resulting dispersion was subsequently centrifuged at 6500 rpm for 20 min to remove the unbound Cap-DNA, and this step was repeated three times. Finally, the remained solution in the centrifuge tube was diluted to 500 μL with PBS. The streptavidin-biotin-Con-DNA conjugates were prepared by employing the same procedure.

Preparation of LFNABs

The LFNAB mainly composed of the following sections: absorbent pad, nitrocellulose membrane, conjugate pad, and sample pad (Scheme 1). Both the absorbent pad and sample pad were cut into 17 mm × 300 mm. The sample pad was treated with a buffer containing 0.15 mM NaCl, 2.5% Tween-20, 0.25% Triton X-100, and 0.05 M Tris–HCl (pH 8.0) and then dried at 37 °C for 12 h and followed by storing at 4 °C. The control and test region of the LFNAB were separately prepared by dispensing the specified volumes of streptavidin-biotinylated Con-DNA (control region) and streptavidin-biotinylated Cap-DNA (test region) solutions on the nitrocellulose membrane (25 mm × 300 mm). The interval between the control and test region was roughly 4 mm, and the control region was close to the absorbent pad. Then the nitrocellulose membrane was dried at 37 °C for 2 h. The conjugate pad was cut into 17 mm × 300 mm. Finally, the four parts mentioned above were assembled on a PVC cohesive backing (60 mm × 300 mm), and each section was overlapping about 2 mm to guarantee that the sample solution was able to stream through all the sections. Strips were sliced into 3.5 mm width on the guillotine cutting module CM3010.

Assay procedure

2.5 μL of AuNR-Det-DNA conjugate was dropped on the conjugate pad. 100 μL sample solution prepared in the running buffer (2% BSA + 1/4 SSC + 1% PVP) was applied to the absorbent pad of the LFNAB. The test and control bands could be observed with the naked eye within 10 min. The density (peak areas) of control and test bands was measured by a portable strip reader for quantitative analysis. Digital images of the LFNABs were captured by camera and then transferred to a computer for processing. Photoshop was used to intercept the C and T lines of the nitrocellulose membrane in the digital images and arrange them neatly for better comparison.

Results and discussion

Characterization of the AuNRs

The AuNRs with three aspect ratios were prepared and characterized by TEM and UV-vis absorption spectra. Figure 1A to C show typical TEM images of AuNRs with aspect ratios of 3.13 (AuNRs-25, A), 2.14 (AuNRs-60, B) and 8.0 (AuNRs-80, C). One hundred nanorods in the images were used to calculate data. One can see that the sizes (length and width) and distributions of the AuNRs are uniform. Figure 1D displays the UV-vis absorption spectra of AuNRs with three aspect ratios. A characteristic absorption peak at approximately 520 nm is observed in the spectra of all three AuNRs, and

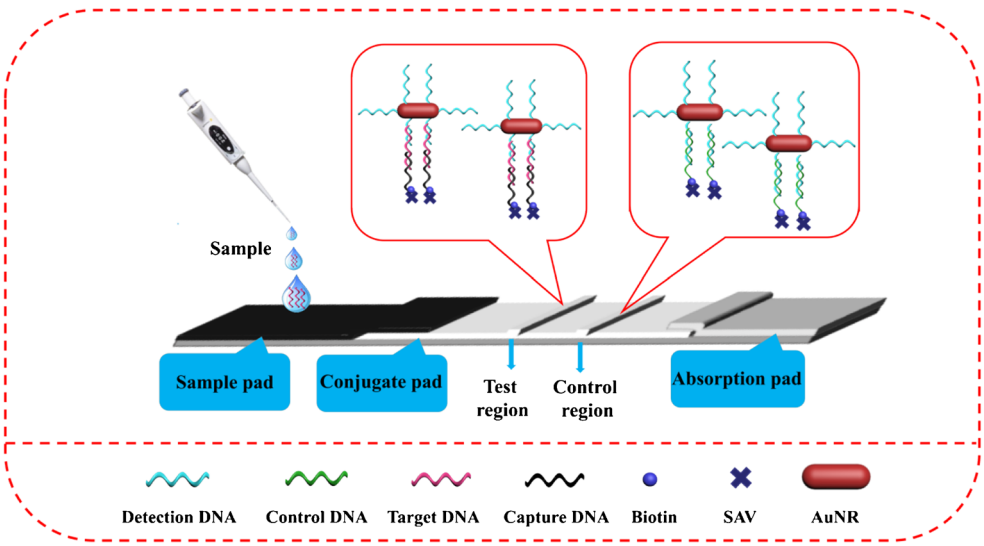

Scheme 1 Schematic illustration of the configuration and measurement principle of the AuNRs-based lateral flow nucleic acid biosensor. SAV, streptavidin

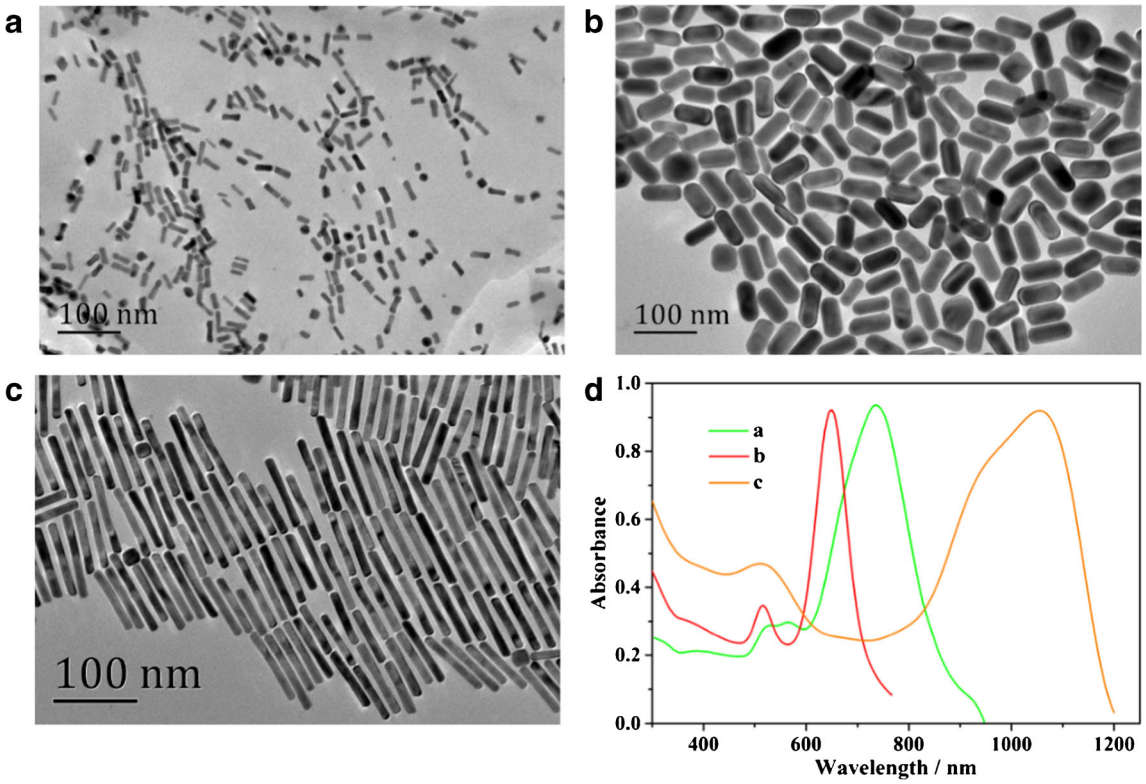

Fig. 1 (**A**) TEM images of AuNRs-25, (**B**) AuNRs-60, (**C**) AuNRs-80, and (**D**) absorption spectra of AuNRs solution with different aspect ratios: a-AuNRs-25, b-AuNRs-60, c-AuNRs-80

longitudinal peaks appear at about 780 nm (AuNRs-25), 620 nm (AuNRs-60), and 1080 nm (AuNRs-80), respectively. The wavelengths of the absorption peaks are consistent with that reported in the previous literatures [34–36].

Working principles of the AuNR-based LFNAB

The working principles of AuNR-based LFNAB stand on the theory of Watson-Crick base-pairing among three DNA probes and target DNA on the test and control regions of LFNAB (Scheme 1). Three DNA probes including a detection DNA (Det-DNA) probe, capture DNA (Cap-DNA) probe, and control DNA (Con-DNA) probe were utilized to prepare the LFNAB. At two ends of the Tar-DNA, the Cap-DNA and Det-DNA are complementary with it, respectively. The Det-DNA probe was linked with AuNR by Au-S bond, and the AuNR-Det-DNA conjugate was dropped on the conjugate pad. Streptavidin was carried out to couple with biotin-modified Cap-DNA firstly, and the obtained streptavidin-biotin-Cap-DNA complex was sprayed onto the LFNAB to build the test region. And the Con-DNA, which is completely complementary to Det-DNA, was sprayed onto the LFNAB to build a control region. In the typical test, the sample solution containing Tar-DNA was applied to the sample pad. The solution could migrate along the strip to the absorbent pad under capillary force, and AuNR-Det-DNA-Tar-DNA complex was formed via the principle of base pairing happening between the Tar-DNA and the Det-DNA probes coupled to AuNR. Upon arriving at the test region, AuNR-Det-DNA-Tar-DNA formed a sandwich-type complex (named AuNR-Det-DNA-Tar-DNA-Cap-DNA) due to another base pairing reactions between the Tar-DNA and Cap-DNA. Accumulation of AuNRs on the test region could produce a characteristic color band (test line) and the density of the band would rise in proportion to the amount of the captured AuNRs, thus to the concentration of Tar-DNA in the sample solution. The excessive AuNR-Det-DNA conjugates continued to move to the control region and are seized by the Con-DNA to produce a second color band (control line). The control line was utilized to affirm whether the LFNAB works regularly. Sandwich-type complexes were not generated on the test region within the nonappearance of Tar-DNA, and only the AuNR-Det-DNA-Con-DNA complex was captured on the control region to produce the control line. The test line could be utilized to determinate the concentration of Tar-DNA qualitatively and quantitatively. The qualitative analysis was easily achieved via the color variation observed on the test region, and the quantitative determination could be established by measuring the strength of test band using a portable strip reader. The sample solution was checked on the traditional AuNPs-based LFNAB and AuNRs (with different aspect ratios)-based LFNABs to verify the proposed signaling strategy obtained

via using AuNRs as colored tags for visible detection of Tar-DNA. Figure 2 displays the typical photograph of AuNP-based LFNABs (Fig. 2a) and AuNR-based LFNABs (Fig. 2b–d) after detecting 0 and 0.2 nM Tar-DNA. In the existence of 0.2 nM Tar-DNA, the AuNP-based LFNAB exhibits a scarcely visible test band (Fig. 2a, right), whereas all the AuNR-based LFNABs exhibit the test lines with different intensities. The AuNR-25-based LFNAB (Fig. 2b, right) and the AuNR-80-based LFNAB(Fig. 2d, right) show weak test lines, whereas AuNR-60-based LFNAB shows a prominent test line (Fig. 2c, right). There is no visible line on the test region of all LFNABs (left LFNAB) when the target DNA is absent. It turned out that the AuNRs might be utilized as colored tags for the visual detection of DNA on the LFNAB and the AuNR-60 shows the best sensitivity. Therefore, the AuNR-60 was chosen as label to prepare the LFNABs for subsequent experiments.

Optimization of analytical parameters

The preparation of AuNR-based LFNABs and experimental parameters employed in the lateral flow assay strongly affected the analytical performance of the LFNABs. To get the best reproducibility and sensitivity of the Tar-DNA detection, we optimized certain features: (a) concentration of SSC running buffer, (b) concentration of PVP added to the SSC running buffer, (c) the concentrations of Det-DNA probe coupled to AuNRs, (d) the dosages of the AuNR-Det-DNA complexes dropped on the conjugate pad, and (e) the dosages of the streptavidin-biotinylated Cap-DNA on the test region. Optimization was carried out by varying one condition and other conditions unchanged, and the analytical performances of the LFNABs were evaluated by signal-to-noise (S/N) ratios. A detailed discussion, the data obtained, and relevant figures were given in the ESM (Fig. S2). The best results were obtained by using the following experimental conditions: (a) 1 × 4 SSC as a running buffer, (b) addition of 1% PVP to the SSC running buffer, (c) use of the 1.5 OD Det-DNA probe to prepare the AuNR-Det-DNA conjugate, (d) use of 6 μL of the AuNR-Det-DNA conjugates per assay, and (e) dispensing of streptavidin-biotinylated Cap-DNA probe four times on the test region.

Analytical performance

The analytical performance of LFNAB which was based on AuNR under various concentration of Tar-DNA was evaluated through the optimized experimental parameters. The captured AuNR gathers in the test region and forms visible color bands for qualitative analysis. For quantitative analysis, a portable strip reader was used to measure the density of the color bands that was proportional to the Tar-DNA concentration. Figure 3a exhibits the graphics of AuNR-based LFNABs (top) under different concentrations of Tar-DNA and the related optical responses of the test lines (bottom). As shown in Fig. 3a, the density of the test band enhanced with the increasing concentration of Tar-DNA. All LFNABs displayed a colored control line, indicating the LFNABs run in fine conditions. In the blank experimental group, known as the control group, the concentration of Tar-DNA was 0 nM. There is no distinct color band on the test region in the blank experimental group, demonstrating insignificant nonspecific adsorption under the optimized test conditions. Moreover, the test band remained relatively clear even when the concentration of target DNA was only 10 pM. Figure 3b displays a calibration curve of the peak area versus the logarithm of Tar-DNA concentration. The logarithm of the different concentrations of Tar-DNA (0.01–10 nM) and the peak area value show a good linear relationship. In addition, the linear regression equation is $y = (429 \pm 20)\ x + (805 \pm 30)$ (y stands for the peak area, x stands for the Tar-DNA concentration) with a coefficient of determination ($R^2 = 0.984$), and the detection limit is 2 pM ($S/N = 3$). The detection time only takes about 10 min. The detection limit of the AuNR-based LFNAB is 250-fold lower than that of the AuNP-based LFNAB. [37] Table 1 compares the detection limits of LFNABs based on diverse nano-labels previously reported. The detection limit of LFNAB based on AuNR shows significant improvement over that acquired from previous reports without signal amplification. The surface of gold nanorods has CTAB as a stabilizer, which enables the gold nanorods has higher stability than colloidal gold and avoids the aggregation issue during the preparation of conjugates. Although it has been reported that using enzyme-loaded colloidal gold as a label to improve the detection limit by enzyme catalytic amplification [19], AuNR as a label can

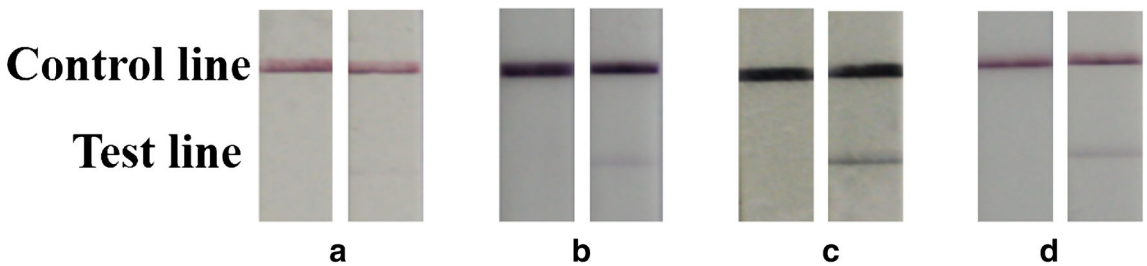

Fig. 2 Photo images of LFNABs using AuNP (**a**), AuNRs-25 (**b**), AuNRs-60 (**c**), and AuNRs-80 (**d**) as colored tags after testing 0 nM (left) and 0.2 nM (right) Tar-DNA

Table 1 Detection limits of LFNABs based on different nano-labels

Reference	Target/label	Detection Limit
[37]	DNA/gold nanoparticle	0.5 nM
[38]	DNA/dye entrapping liposome	1.0 nM
[39]	microRNA/gold nanoparticle	60 pM
[26]	DNA/molecular beacon functionalized gold nanoparticle	50 pM
[4]	DNA/carbon nanotube based lateral flow biosensor	40 pM
[20]	microRNA/gold nanoparticle coated silica nanorod	10 pM
[19]	DNA/gold nanoparticle-horseradish peroxidase	1.25 fM
This work	DNA/gold nanorods	2.0 pM

directly lower the detection limit without any signal amplification process.

The selectivity of AuNR-based LFNABs were evaluated by comparing the responses of complementary Tar-DNA and mismatched DNAs including one-base mismatched DNA (OM-DNA), two-base mismatched DNA (TM-DNA), and non-complementary DNA (NC-DNA) (ESM, Fig. S3).

The results showed that the S/N ratio of 0.5 nM complementary Tar-DNA is eight times more than that of 0.5 nM OM-DNA, 5 nM TM-DNA, and 5 nM NC-DNA. Consequently, OM-DNA and TM-DNA could be distinguished from the target DNA by the AuNR-based LFNAB. The reproducibility of AuNR-based LFNAB was examined by testing against 0, 0.05, and 2.0 nM target DNA. Samples at each concentration level was examined six times with six LFNABs and the corresponding relative standard deviations of the responses were 0.21%, 6.1%, and 4.3% respectively, which implied prominent analytical reproducibility.

To evaluate the applicability of LFNAB detecting DNA in biological matrices, recovery experiment was further

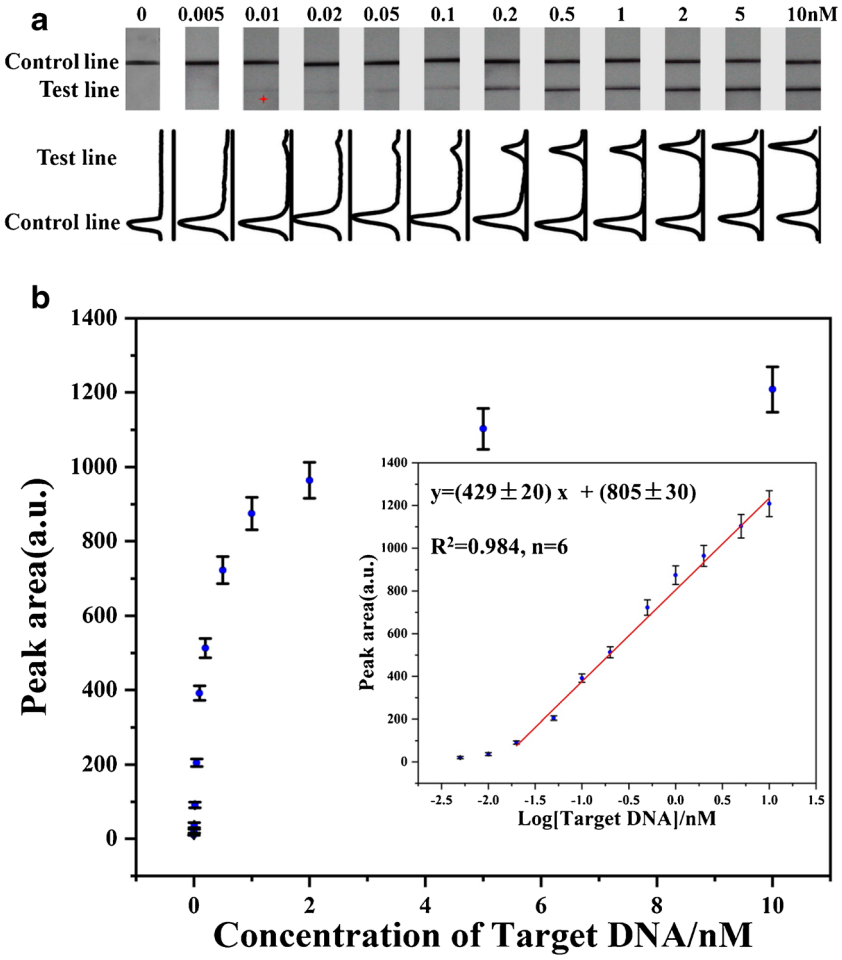

Fig. 3 (**a**) Images of the LFNABs and the test band intensity responses acquired from the strip reader under different concentration Tar-DNA. The asterisks (+) show the detection limit of LFNABs by the naked eyes. (**b**) Typical dot plot and calibration curve (the inset) of the peak area versus the logarithm of target DNA concentration. Error bars indicate standard deviations of six independent measurements

Table 2 The recovery of LFNAB for testing DNA in spiked serum

Sample Number	Spiked concentration (pM)	Measured concentration (pM)	Recovery (%)	Relative standard deviation (%, n=6)
1	50	46	92.0	6.8
2	500	478	95.6	4.2
3	5000	5155	103.1	4.3

investigated. A series of Tar-DNA concentrations (0, 50, 500, and 5000 pM) were spiked into diluted serum at equal volumes. The recoveries ranged from 92.0 to 103.1% as presented in Table 2. The results indicate that the detection is less influenced by the matrix in biological samples.

Conclusion

The present study describes an AuNR-based lateral flow nucleic acid biosensor for the fast and sensitive detection of DNA. After systematic optimizations, a linear dynamic range of 0.01–10 nM and LOD of 2 pM was obtained for the detection of DNA without any signal amplification process. Moreover, good performance was obtained in single-nucleotide polymorphism detection and spiked serum samples. Although AuNR shows good performance, precise control of aspect ratio and batch preparation are still challenging. In addition, the LOD of current work is not enough to detect nucleic acids (DNA and microRNA) directly in complex biological samples, and future work will aim to integrate isothermal nucleic acid amplification techniques with the gold nanorods-based lateral flow biosensors for ultrasensitive detection of nucleic acids in clinical samples. We will explore the multiplex capability of gold nanorods and excavate its meaningful applications in clinic diagnosis.

Supplementary Information The online version contains supplementary material available at https://doi.org/10.1007/s00604-021-04788-z.

Funding This study received funding from the Natural Science Foundation of Anhui province (Nos. 1808085QH264, 1908085MB54), Key Research and Development Projects of Anhui Province (No. 202004a07020018), Major project of Anhui Provincial Department of Education (No. KJ2019ZD58), and Wanjiang Scholar Award of Anhui Province, National Natural Science Foundation of China (Nos. 31700735, 21890740, 21890742, 21727815). Projects of Anhui Science and Technology University for Talent introduction (SKYJ201903).

Declarations

Conflict of interest The author(s) declare that they have no competing interests.

References

1. Corstjens P, Zuiderwijk M, Brink A, Li S, Feindt H, Niedbala RS, Tanke H (2001) Use of up-converting phosphor reporters in lateral-flow assays to detect specific nucleic acid sequences: a rapid, sensitive DNA test to identify human papillomavirus type 16 infection. Clin Chem 47(10):1885–1893
2. Mao X, Xu H, Zeng Q, Zeng L, Liu G (2009) Molecular beacon-functionalized gold nanoparticles as probes in dry-reagent strip biosensor for DNA analysis. Chem Commun 21:3065–3067
3. Zhao X, Tapec-Dytioco R, Tan W (2003) Ultrasensitive DNA detection using highly fluorescent bioconjugated nanoparticles. J Am Chem Soc 125(38):11474–11475
4. Qiu W, Xu H, Takalkar S, Gurung AS, Liu B, Zheng Y, Guo Z, Baloda M, Baryeh K, Liu G (2015) Carbon nanotube-based lateral flow biosensor for sensitive and rapid detection of DNA sequence. Biosens Bioelectron 64:367–372
5. Sher M, Zhuang R, Demirci U, Asghar W (2017) Paper-based analytical devices for clinical diagnosis: recent advances in the fabrication techniques and sensing mechanisms. Expert Rev Mol Diagn 17(4):351–366
6. Rahman M, Uddin M, Sultana R, Moue A, Setu M (2013) Polymerase chain reaction (PCR): a short review. Anwer Khan Modern Medical College Journal 4:30–36
7. Seki Y, Fujiwara Y, Kohno T, Takai E, Sunami K, Goto Y, Horinouchi H, Kanda S, Nokihara H, Watanabe S, Ichikawa H, Yamamoto N, Kuwano K, Ohe Y (2016) Picoliter-droplet digital polymerase chain reaction-based analysis of cell-free plasma DNA to assess EGFR mutations in lung adenocarcinoma that confer resistance to tyrosine-kinase inhibitors. Oncologist 21(2):156–164
8. Porter-Jordan K, Rosenberg EI, Keiser JF, Gross JD, Ross AM, Nasim S, Garrett CT (1990) Nested polymerase chain reaction assay for the detection of cytomegalovirus overcomes false positives caused by contamination with fragmented DNA. J Med Virol 30(2): 85–91
9. Takalkar S, Baryeh K, Liu G (2017) Fluorescent carbon nanoparticle-based lateral flow biosensor for ultrasensitive detection of DNA. Biosens Bioelectron 98:147–154
10. Khlebtsov BN, Bratashov DN, Byzova NA, Dzantiev BB, Khlebtsov NG (2019) SERS-based lateral flow immunoassay of troponin I by using gap-enhanced Raman tags. Nano Res 12(2): 413–420
11. Ren W, Mohammed SI, Wereley S, Irudayaraj J (2019) Magnetic focus lateral flow sensor for detection of cervical cancer biomarkers. Anal Chem 91(4):2876–2884
12. Fu X, Cheng Z, Yu J, Choo P, Chen L, Choo J (2016) A SERS-based lateral flow assay biosensor for highly sensitive detection of HIV-1 DNA. Biosens Bioelectron 78:530–537
13. He Y, Zeng K, Gurung AS, Baloda M, Xu H, Zhang X, Liu G (2010) Visual detection of single-nucleotide polymorphism with hairpin oligonucleotide-functionalized gold nanoparticles. Anal Chem 82(17):7169–7177

14. Hwang J, Kwon D, Lee S, Jeon S (2016) Detection of Salmonella bacteria in milk using gold-coated magnetic nanoparticle clusters and lateral flow filters. RSC Adv 6(54):48445–48448
15. Wen H-W, Borejsza-Wysocki W, DeCory TR, Durst RA (2005) Development of a competitive liposome-based lateral flow assay for the rapid detection of the allergenic peanut protein Ara h1. Anal Bioanal Chem 382(5):1217–1226
16. Wang J, Cao F, He S, Xia Y, Liu X, Jiang W, Yu Y, Zhang H, Chen W (2018) FRET on lateral flow test strip to enhance sensitivity for detecting cancer biomarker. Talanta 176:444–449
17. Gao Y, Deng X, Wen W, Zhang X, Wang S (2017) Ultrasensitive paper based nucleic acid detection realized by three-dimensional DNA-AuNPs network amplification. Biosens Bioelectron 92:529–535
18. Peng T, Wang J, Zhao S, Zeng Y, Zheng P, Liang D, Mari GM, Jiang H (2018) Highly luminescent green-emitting Au nanocluster-based multiplex lateral flow immunoassay for ultrasensitive detection of clenbuterol and ractopamine. Anal Chim Acta 1040:143–149
19. He Y, Zhang S, Zhang X, Baloda M, Gurung AS, Xu H, Zhang X, Liu G (2011) Ultrasensitive nucleic acid biosensor based on enzyme–gold nanoparticle dual label and lateral flow strip biosensor. Biosens Bioelectron 26(5):2018–2024
20. Takalkar S, Xu H, Chen J, Baryeh K, Qiu W, Zhao JX, Liu AG (2016) Gold nanoparticle coated silica nanorods for sensitive visual detection of microRNA on a lateral flow strip biosensor. Anal Sci 32(6):617–622
21. Elahi N, Kamali M, Baghersad MH (2018) Recent biomedical applications of gold nanoparticles: a review. Talanta 184:537–556
22. Cao J, Sun T, Grattan KTV (2014) Gold nanorod-based localized surface plasmon resonance biosensors: a review. Sensors Actuators B Chem 195:332–351
23. Locatelli E, Monaco I, Comes Franchini M (2015) Surface modifications of gold nanorods for applications in nanomedicine. RSC Adv 5(28):21681–21699
24. Xu L, Kuang H, Wang L, Xu C (2011) Gold nanorod ensembles as artificial molecules for applications in sensors. J Mater Chem 21(42):16759–16782
25. Kabashin AV, Evans P, Pastkovsky S, Hendren W, Wurtz GA, Atkinson R, Pollard R, Podolskiy VA, Zayats AV (2009) Plasmonic nanorod metamaterials for biosensing. Nat Mater 8(11):867–871
26. Yu C, Irudayaraj J (2007) Multiplex biosensor using gold nanorods. Anal Chem 79(2):572–579
27. Hao K, He Y, Lu H, Pu S, Zhang Y, Dong H, Zhang X (2017) High-sensitive surface plasmon resonance microRNA biosensor based on streptavidin functionalized gold nanorods-assisted signal amplification. Anal Chim Acta 954:114–120
28. Li Y, Zhang Y, Zhao M, Zhou Q, Wang L, Wang H, Wang X, Zhan L (2016) A simple aptamer-functionalized gold nanorods based biosensor for the sensitive detection of MCF-7 breast cancer cells. Chem Commun 52(20):3959–3961
29. Zhu W, Xuan C, Liu G, Chen Z, Wang W (2015) A label-free fluorescent biosensor for determination of bovine serum albumin and calf thymus DNA based on gold nanorods coated with acridine orange-loaded mesoporous silica. Sensors Actuators B Chem 220:302–308
30. Li C-Z, Male KB, Hrapovic S, Luong JHT (2005) Fluorescence properties of gold nanorods and their application for DNA biosensing. Chem Commun 31:3924–3926
31. Shakoori Z, Salimian S, Kharrazi S, Adabi M, Saber R (2015) Electrochemical DNA biosensor based on gold nanorods for detecting hepatitis B virus. Anal Bioanal Chem 407(2):455–461
32. Xu C, Lan L, Yao Y, Ping J, Li Y, Ying Y (2018) An unmodified gold nanorods-based DNA colorimetric biosensor with enzyme-free hybridization chain reaction amplification. Sensors Actuators B Chem 273:642–648
33. Tao Y, Yang J, Chen L, Huang Y, Qiu B, Guo L, Lin Z (2018) Dialysis assisted ligand exchange on gold nanorods: amplification of the performance of a lateral flow immunoassay for *E. coli* O157:H7. *Microchimica Acta 185*(7):350
34. Nikoobakht B, El-Sayed MA (2003) Preparation and growth mechanism of gold nanorods (NRs) using seed-mediated growth method. Chem Mater 15(10):1957–1962
35. Sau TK, Murphy CJ (2004) Seeded high yield synthesis of short Au nanorods in aqueous solution. Langmuir 20(15):6414–6420
36. Vigderman L, Zubarev ER (2013) High-yield synthesis of gold nanorods with longitudinal SPR peak greater than 1200 nm using hydroquinone as a reducing agent. Chem Mater 25(8):1450–1457
37. Mao X, Ma Y, Zhang A, Zhang L, Zeng L, Liu G (2009) Disposable nucleic acid biosensors based on gold nanoparticle probes and lateral flow strip. Anal Chem 81(4):1660–1668
38. Baeumner AJ, Pretz J, Fang S (2004) A universal nucleic acid sequence biosensor with nanomolar detection limits. Anal Chem 76(4):888–894
39. Gao X, Xu H, Baloda M, Gurung AS, Xu L-P, Wang T, Zhang X, Liu G (2014) Visual detection of microRNA with lateral flow nucleic acid biosensor. Biosens Bioelectron 54:578–584